Bull. Chem. Soc. Ethiop. **2026**, 40(1), 147-157.
DOI: https://dx.doi.org/10.4314/bcse.v40i1.12
© 2025 Chemical Society of Ethiopia and The Authors
ISSN 1011-3924
Printed in Ethiopia
Online ISSN 1726-801X

NEUROPROTECTIVE POTENTIAL OF SECONDARY METABOLITES FROM *TRICHODERMA KONINGIOPSIS* YN-G-1, AN ENDOPHYTIC FUNGUS OF THE ENDANGERED PLANT *TAXUS YUNNANENSIS*

Xin Chen[1], Zhong-Duo Yang[1*], Wen-Lin Guo[1, 2], Ke-Zhen Ma[1], Jian-Guo Chen[1]

[1]School of Life Science and Engineering, Lanzhou University of Technology, Lanzhou 730050, People's Republic of China
[2]Wenzhou Engineering Institute of Pump & Valve, Lanzhou University of Technology

(Received April 10, 2025; Revised July 24, 2025; Accepted October 8, 2025)

ABSTRACT. Endophytic fungi in endangered plants produce bioactive metabolites with neuroprotective potential. In this study, eight secondary metabolites were isolated from *Trichoderma koningiopsis* YN-G-1 (endophyte of *Taxus yunnanensis*) using ethyl acetate extraction and chromatographic fractionation. Structures were elucidated by NMR spectroscopy and corroborated with literature data. Activity screening demonstrated that trichodermaketone C (**4**) effectively inhibits AChE (IC_{50} = 4.3 μM), PI3K (IC_{50} = 0.15 μM), and PDE1 (IC_{50} = 56.5 μM), suggesting multi-target neuroprotective effects. This work expands the chemical diversity of *T. koningiopsis* and highlights its promise for neurodegenerative drug discovery.

KEY WORDS: *Taxus yunnanensis*, *Trichoderma koningiopsis*, Secondary metabolites, Polyketides, Neuroprotective potential

INTRODUCTION

Conifers (Pinopsida: Gymnospermae) represent an evolutionarily significant plant group comprising several ecologically and economically important families, such as Pinaceae, Taxaceae, Podocarpaceae, Araucariaceae, and Cephalotaxaceae [1]. Among these, *Taxus yunnanensis* (Taxaceae) stands out as a critically endangered conifer of exceptional pharmaceutical importance. This species has become a focal point in biomedical research owing to its biosynthetic capacity to produce paclitaxel, a diterpenoid-derived alkaloid widely used in cancer chemotherapy, and pharmacologically active heteropolysaccharides with demonstrated antitumor and immunomodulatory properties [2]. Notably, the ecological significance of endangered plants extends beyond their intrinsic bioactive compounds, as they maintain highly specialized symbiotic relationships with diverse endophytic communities. These unique microbiomes, shaped by coevolutionary processes within distinct ecological niches, have demonstrated remarkable metabolic capabilities, including the biosynthesis of secondary metabolites structurally and functionally analogous to those produced by their host plants, thereby offering new avenues for natural product discovery and biotechnological applications [3-6].

Current research has made substantial progress in investigating secondary metabolites derived from microbial communities associated with rare and endangered coniferous species. In 2023, Chen *et al.* conducted a comprehensive study on endophytic fungi isolated from the foliage of *Pseudotsuga gaussenii* (Pinaceae), a vulnerable species endemic to Mount Sanqing in Jiangxi Province. Their work encompassed fungal isolation, taxonomic identification, and metabolic profiling of target strains. From the *Phyllosticta ligustricola* HDF-L-2 strain, five monomeric

*Corresponding author. E-mail: yangzhongduo@126.com
This work is licensed under the Creative Commons Attribution 4.0 International License

secondary metabolites were successfully isolated, all identified as spirobisnaphthalene-type polyketides. Notably, four novel compounds were characterized, including three unprecedented spirobisnaphthalene derivatives fused with pyranone moieties. Pharmacological evaluations revealed significant biological activities, including antimicrobial effects, cytotoxicity, and dual inhibition of ACL (ATP-citrate lyase) and ACC1 (acetyl-CoA carboxylase 1) enzymes [7]. Advancing this field, Quyet-Tien Phi *et al.* (2024) isolated 16 endophytic fungal strains (representing seven genera, including *Fusarium*, *Penicillium*, and *Aspergillus*) from *Amentotaxus yunnanensis*. Preliminary screening identified *Fusarium foetens* A QF6 crude extract as exhibiting remarkable chemical diversity and potent radical-scavenging capacity. Large-scale fermentation of this strain yielded 15 purified compounds, featuring a novel bisabolane-type sesquiterpenoid alongside 14 known metabolites spanning diverse structural classes (polyketides, nucleosides, and alkaloids). The novel sesquiterpenoid demonstrated exceptional antioxidant efficacy in DPPH and ABTS radical scavenging assays [8]. These findings collectively demonstrate that endophytic fungi associated with rare and endangered coniferous species possess substantial potential and significant value for the discovery of novel chemical entities and innovative therapeutic agents with unique mechanisms of action [9, 10].

Conversely, *T. koningiopsis* (Ascomycota: Hypocreaceae) has attracted scientific interest due to the structural novelty and chemical diversity of its secondary metabolites, which frequently exhibit a wide range of bioactivities, including antimicrobial and anti-inflammatory properties [11]. In a pioneering study, Hu *et al.* isolated two novel polyketide derivatives, koninginins R and S, from the endophytic fungal strain *T. koningiopsis* YIM PH30002 associated with *Panax notoginseng*. Both compounds demonstrated significant antifungal activity against the phytopathogenic fungal species *Fusarium flocciferum* and *Fusarium oxysporum* [12]. Subsequently, Shi et al. expanded the chemical diversity of this genus by characterizing eight new highly oxygenated polyketides from the fermentation extract of *T. koningiopsis* QA-3 derived from *Artemisia argyi* [13]. Further contributing to this chemical repertoire, Lang *et al.* reported two additional polyketides, koninginins L and M, from the fermentation extract of *T. koningii* 8662 [14].

In summary, this study focuses on endophytic fungi associated with endangered coniferous plants, specifically investigating the secondary metabolites and biological activities of *T. koningiopsis* strain YN-G-1 isolated from *Taxus yunnanensis*. The research aims to discover novel structural classes of bioactive compounds, thereby expanding the repertoire of natural products with potential pharmacological applications.

RESULTS AND DISCUSSION

In this study, eight secondary metabolites were isolated from the endophytic fungus *T. koningiopsis* YN-G-1 derived from *Taxus yunnanensis*. Structural characterization identified these compounds as koninginin A (**1**), koninginin D (**2**), trichodermatide B (**3**), trichodermaketone C (**4**), koninginin B (**5**), ergosterol peroxide (**6**), p-hydroxyphenyl-β-ethanol (**7**), and drechslerol B (**8**). All compounds were characterized through spectroscopic data analysis and comparison with literature reports. Their chemical structures are presented in Figure 1.

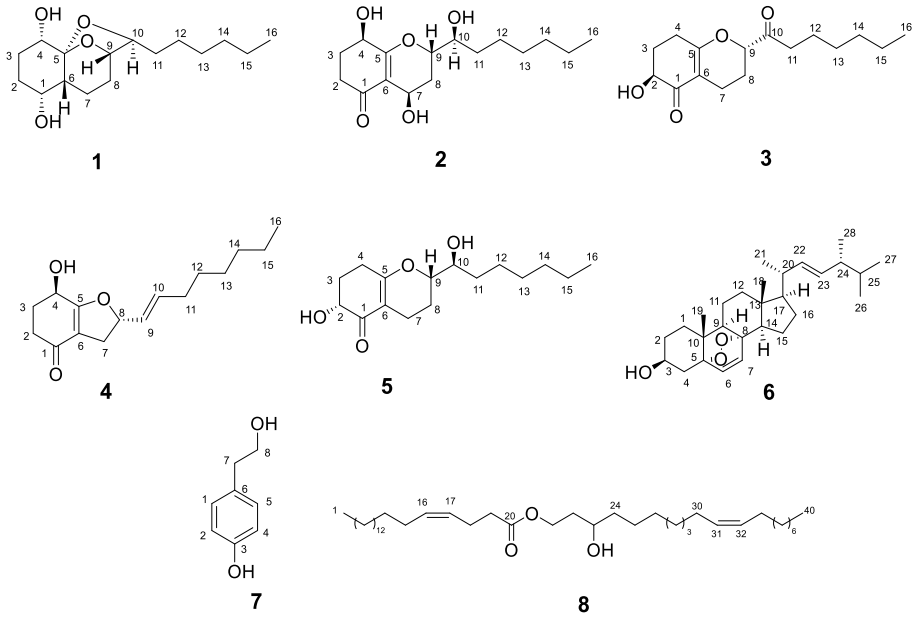


Figure 1. Structures of compounds **1**-**8**.

Compound **1** was identified as koninginin A [15], and its structure was confirmed by comprehensive NMR analysis. The ^{1}H-NMR spectrum (600 MHz, $CDCl_3$) exhibited signals for four oxygenated methine protons at δ_H 4.31 (1H, br s, H-9), 4.02 (1H, t, J = 7.0 Hz, H-10), 3.88 (1H, ddd, J = 11.3, 5.0, 3.1 Hz, H-1), and 3.61 (1H, dd, J = 11.9, 4.2 Hz, H-4). Additional proton signals included multiplets at δ_H 2.25 (1H, m, H-8b), 2.09 (1H, m, H-7a), 1.96 (1H, m, H-3b), 1.86 (1H, m, H-3a), 1.81 (1H, m, H-2b), 1.71 (1H, m, H-7b), 1.58 (1H, m, H-2a), 1.57 (1H, m, H-6), 1.52 (1H, m, H-11a), 1.50 (1H, m, H-8a), and 1.48 (1H, m, H-11b), along with a broad multiplet at δ_H 1.31 (8H, m, H-12,13,14,15) and a terminal methyl triplet at δ_H 0.87 (3H, t, J = 6.9 Hz, H-16). The ^{13}C-NMR spectrum (150 MHz, $CDCl_3$) revealed characteristic carbon resonances, including a ketal carbon at δ_C 109.4 (C-5), oxygenated methine carbons at δ_C 79.5 (C-10), 79.3 (C-9), 72.9 (C-1), and 70.1 (C-4), methylene carbons at δ_C 41.6 (C-6), 35.4 (C-11), 31.9 (C-14), 31.0 (C-2), 29.2 (C-13), 27.4 (C-8), 25.7 (C-12), 25.4 (C-3), 22.7 (C-15), and 20.7 (C-7), and a terminal methyl carbon at δ_C 14.2 (C-16).

Compound **2** was identified as koninginin D [16], and its structure was elucidated through detailed NMR analysis. The ^{1}H-NMR spectrum (600 MHz, $CDCl_3$) showed characteristic signals for four oxygenated methine protons at δ_H 4.67 (1H, s, H-7), 4.37 (1H, d, J = 6.0 Hz, H-4), 3.78 (1H, s, H-9), and 3.62 (1H, s, H-10). Additional proton signals included methylene multiplets at δ_H 2.60 (1H, dq, J = 16.8, 6.8 Hz, H-2b), 2.44 (1H, d, J = 16.8 Hz, H-2a), 2.29 (1H, ddt, J = 14.2, 6.0, 2.2 Hz, H-3b), 2.19 (1H, m, H-3a), 2.07 (1H, ddd, J = 12.7, 4.4, 2.2 Hz, H-8b), 1.96 (1H, d, J = 14.2 Hz, H-8a), 1.51 (4H, m, H-11, 12), 1.37 (2H, m, H-13), along with merged aliphatic signals at δ_H 1.26 (6H, m, H-13, 14, 15), and a terminal methyl triplet at δ_H 0.85 (3H, t, J = 6.8 Hz, H-16). The ^{13}C-NMR spectrum (150 MHz, $CDCl_3$) revealed key carbon resonances, including a ketone carbonyl at δ_C 197.9 (C-1), conjugated double bond carbons at δ_C 169.8 (C-5) and 111.3 (C-6), oxygenated methine carbons at δ_C 81.5 (C-9), 73.6 (C-10), 66.0 (C-4), and 50.7 (C-7), methylene carbons at δ_C 33.5 (C-2), 32.7 (C-8), 31.9 (C-11), 29.4 (C-13), 29.2 (C-14), 25.2 (C-12), 22.9 (C-3), 22.7 (C-15), and a terminal methyl carbon at δ_C 14.2 (C-16).

Compound **3** was identified as trichodermatides B [17], and its structure was fully characterized by NMR spectroscopy. The ^{1}H-NMR spectrum (600 MHz, $CDCl_3$) displayed characteristic signals including an oxygenated methine proton at δ_H 5.25 (1H, m, H-9), another oxygenated methine proton at δ_H 4.05 (1H, m, H-2), multiple methylene protons between δ_H 3.12-2.38 (assigned to H-8, H-7α, H-7β, H-4, H-11), a methylene multiplet at δ_H 2.35 (1H, m, H-3α), δ_H 1.84 (1H, m, H-3β), δ_H 1.54 (2H, m, H-12), δ_H 1.23 (6H, br s, H-13,14,15), and a terminal methyl triplet at δ_H 0.83 (3H, t, J = 6.8 Hz, H-16). The ^{13}C-NMR spectrum (150 MHz, $CDCl_3$) revealed two carbonyl carbons at δ_C 207.4 (10-CO) and 195.1 (1-CO), conjugated double bond carbons at δ_C 177.8 (C-5) and 110.6 (C-6), oxygenated carbons at δ_C 82.3 (C-9) and 71.5 (C-2), methylene carbons at δ_C 48.4 (C-8), 43.5 (C-11), 31.7 (C-7), 31.6 (C-14), 30.1 (C-3), 28.8 (C-13), 23.5 (C-12), 22.9 (C-4), and 22.5 (C-15), with a terminal methyl carbon at δ_C 14.0 (C-16).

Compound **4** was identified as trichodermaketone C [18], and its structure was fully characterized by NMR spectroscopy. The ^{1}H-NMR spectrum (600 MHz, $CDCl_3$) exhibited characteristic signals for olefinic protons at δ_H 5.54 (1H, dt, J = 14.8, 6.7 Hz, H-10) and δ_H 5.32 (1H, dd, J = 15.1, 7.8 Hz, H-9), along with an oxygenated methine proton at δ_H 4.96 (1H, m, H-8) and another oxygenated methine proton at δ_H 4.31 (1H, t, J = 6.7 Hz, H-4). Additional signals included methylene protons at δ_H 2.73 (1H, dd, J = 14.8, 9.9 Hz, H-7a), δ_H 2.36 (1H, dd, J = 14.8, 7.8 Hz, H-7b), δ_H 2.31 (1H, m, H-2a), δ_H 2.11 (1H, m, H-2b), δ_H 2.03 (1H, m, H-3a), δ_H 1.81 (2H, m, H-11), δ_H 1.74 (1H, m, H-3b), δ_H 1.12 (2H, m, H-12), δ_H 1.01 (6H, br s, H-13,14,15), and a terminal methyl triplet at δ_H 0.61 (3H, t, J = 6.8 Hz, H-16). The ^{13}C-NMR spectrum (150 MHz, $CDCl_3$) revealed a carbonyl carbon at δ_C 195.1 (1-CO), conjugated double bond carbons at δ_C 175.5 (C-5) and 113.1 (C-6), olefinic carbons at δ_C 136.4 (C-10) and 127.8 (C-9), an oxygenated quaternary carbon at δ_C 87.5 (C-8), an oxygenated methine carbon at δ_C 63.8 (C-4), methylene carbons at δ_C 34.8 (C-2), 32.5 (C-7), 32.2 (C-11), 31.8 (C-13), 31.0 (C-3), 28.9 (C-12), 28.8 (C-14), and 22.7 (C-15), with a terminal methyl carbon at δ_C 14.2 (C-16).

Compound **5** was identified as koninginin B [19], and its structure was fully characterized through detailed NMR analysis. The ^{1}H-NMR spectrum (600 MHz, $CDCl_3$) exhibited characteristic signals for three oxygenated methine protons at δ_H 4.05 (1H, dd, J = 13.1, 5.4 Hz, H-2), 3.78 (1H, ddd, J = 11.3, 5.0, 2.1 Hz, H-9), and 3.64 (1H, dt, J = 7.7, 5.0 Hz, H-10). Additional proton signals included methylene multiplets at δ_H 2.60 (1H, m, H-4b), 2.46 (1H, m, H-4a), 2.36 (1H, m, H-3a), 2.05 (3H, m, H-7, H-8a), 1.79 (1H, m, H-3b), 1.63 (3H, m, H-8b, H-11), along with a broad multiplet at δ_H 1.31 (8H, m, H-12,13,14,15) and a terminal methyl triplet at δ_H 0.88 (3H, t, J = 6.8 Hz, H-16). The ^{13}C-NMR spectrum (150 MHz, $CDCl_3$) revealed key structural features including a ketone carbonyl at δ_C 198.2 (1-CO), conjugated double bond carbons at δ_C 171.4 (C-5) and 109.3 (C-6), oxygenated methine carbons at δ_C 80.9 (C-9), 73.3 (C-10), and 71.2 (C-2), methylene carbons at δ_C 32.9 (C-11), 31.9 (C-14), 29.4 (C-15), 29.1 (C-3), 27.3 (C-4), 25.5 (C-12), 22.8 (C-8), 22.7 (C-15), and 17.8 (C-7), with a terminal methyl carbon at δ_C 14.2 (C-16).

Compound **6** was identified as ergosterol peroxide [20], and its structure was unambiguously characterized by comprehensive NMR analysis. The ^{1}H-NMR spectrum (600 MHz, $CDCl_3$) revealed characteristic signals including olefinic protons at δ_H 6.50 (1H, d, J = 8.5 Hz, H-7) and δ_H 6.23 (1H, d, J = 8.5 Hz, H-6), demonstrating the presence of a conjugated double bond system. Additional olefinic protons appeared at δ_H 5.21 (1H, dd, J = 15.2, 7.7 Hz, H-23) and δ_H 5.14 (1H, dd, J = 15.2, 8.4 Hz, H-22), confirming a trans-disubstituted double bond. The oxygenated methine proton at δ_H 3.97 (1H, m, H-3) indicated hydroxyl substitution at C-3. The methyl groups were observed at δ_H 0.99 (3H, d, J = 6.6 Hz, H-21), δ_H 0.89 (3H, d, J =6.6 Hz, H-28), δ_H 0.87 (3H, s, H-19), δ_H 0.82 (3H, d, J =6.8 Hz, H-27), and δ_H 0.81 (6H, m, H-18, H-26), displaying the characteristic methyl distribution pattern of the steroidal skeleton.

Compound **7** was identified as p-hydroxyphenyl-β-ethanol [21], and its structure was fully characterized by NMR spectroscopy. The ^{1}H-NMR spectrum (600 MHz, CD_3OD) displayed characteristic aromatic proton signals at δ_H 7.04 (2H, d, J = 8.4 Hz, H-2/H-6) and δ_H 6.71 (2H, d,

J = 8.4 Hz, H-3/H-5), showing a typical AA'BB' coupling pattern of a para-substituted benzene ring. The oxymethylene protons appeared as a triplet at δ_H 3.69 (2H, t, *J* = 7.2 Hz, H-8), while the adjacent methylene group resonated at δ_H 2.72 (2H, t, *J* = 7.2 Hz, H-7). The ^{13}C-NMR spectrum (150 MHz, CD_3OD) revealed the aromatic carbons at δ_C 155.3 (C-4, oxygenated quaternary carbon), δ_C 129.6 (C-1), δ_C 129.4 (C-2/C-6), and δ_C 114.7 (C-3/C-5). The aliphatic carbons were observed at δ_C 63.2 (C-8, oxymethylene carbon) and δ_C 38.1 (C-7, methylene carbon).

Compound **8** was identified as Drechslerol B [22], and its structure was fully elucidated through comprehensive NMR analysis. The ^{1}H-NMR spectrum (600 MHz, $CDCl_3$) exhibited characteristic olefinic proton signals at δ_H 5.35 (4H, m, H-16/H-17/H-31/H-32), confirming the presence of two disubstituted double bonds in the structure. The oxymethylene protons appeared at δ_H 4.29 (2H, dd, *J* = 12.0, 4.3 Hz, H-21), while the oxygenated methine proton resonated at δ_H 4.14 (1H, m, H-23). The aliphatic methylene protons showed complex multiplets at δ_H 2.05 (2H, m, H-22) and δ_H 2.01-1.25 (60H, m, representing 30×CH_2 groups in the long aliphatic chains). The terminal methyl groups were observed as a triplet at δ_H 0.87 (6H, t, *J* = 6.8 Hz, H-1/H-40). The ^{13}C-NMR spectrum (150 MHz, $CDCl_3$) revealed the ester carbonyl carbon at δ_C 173.4 (C-20), while the olefinic carbons appeared at δ_C 130.4 (C-16/C-17) and δ_C 130.1 (C-31/C-32). The oxygenated carbons were observed at δ_C 69.0 (C-23) and δ_C 62.2 (C-21). The aliphatic methylene carbons resonated between δ_C 34.2-22.7 (31 carbons), and the terminal methyl carbons appeared at δ_C 14.2 (C-1/C-40).

In summary, the chemical profile of *T. koningiopsis* YN-G-1 was characterized by a predominance of polyketides. These secondary metabolites, biosynthesized from acetyl and malonyl precursors, display complex structural architectures and demonstrate notable bioactivities, including antimicrobial and antioxidant properties. Polyketides serve two significant roles: they are essential for fungal environmental adaptation and competitive survival, while their structural complexity and functional diversity endow them with versatile biological properties. These characteristics make polyketides particularly valuable for pharmaceutical development and highlight their considerable potential as resources for drug discovery and biotechnological applications. To the best of our knowledge, compounds **6** and **8** reported here have been isolated from *T. koningiopsis* for the first time. Compounds **1**, **2**, **3**, **4**, **5,** and **7** have been previously reported from *T. koningiopsis* [16, 18, 23-25].

Notably, structurally diverse polyketides derived from *Trichoderma* spp. have demonstrated potent enzyme inhibitory activities, including monoamine oxidase (MAO) and tyrosine kinase inhibitory effects [26]. This evidence prompted our investigation into the inhibitory potential of the isolated compounds against key therapeutic targets such as MAO, AChE, PI3K, and PDE1. MAO is acknowledged as a viable therapeutic target for pharmacological interventions in depression, anxiety-related disorders, and Parkinson's disease [27]. AChE, an enzyme essential for terminating acetylcholine-mediated neurotransmission, serves as an established pharmacological target in Alzheimer's disease therapy [28]. PI3K, central regulators of cell proliferation and survival, are recognized molecular targets for anticancer drug discovery [29]. PDE1, a modulator of cyclic nucleotide (cAMP/cGMP) metabolism, has garnered attention for its therapeutic relevance in neurological, cardiovascular, and oncological contexts [30].

To identify potential inhibitors of MAO, AChE, PI3K, and PDE1 from natural sources, we systematically evaluated isolated compounds against these enzyme systems. The evaluation revealed that Compound **4** exhibits significant multi-enzyme inhibitory activity, demonstrating effective AChE inhibition (IC_{50} = 4.3 μM), particularly potent PI3K inhibition (IC_{50} = 0.15 μM), and notable PDE1 inhibition (IC_{50} = 56.5 μM). These results indicate Compound **4**'s ability to simultaneously inhibit AChE, PI3K, and PDE1, establishing it as a promising multi-target inhibitor candidate, though further validation of its selectivity and toxicity profile remains essential.

Table 1. IC_{50} values of the tested compounds toward different enzymes.

Compd.	IC_{50} (μM)			
	MAO	AChE	PI3K	PDE1
1	64.4 ±9.7	18.6±2.80	1.41±0.21	>100
2	>100	6.03±0.90	0.67±0.11	>100
3	>100	6.06±0.91	0.71±0.11	63.8±9.6
4	>100	4.30±0.65	0.15±0.02	56.5±8.5
5	>100	14.9±2.20	0.35±0.05	>100
6	>100	12.6±1.90	0.41±0.06	>100
7	>100	34.7±5.20	2.17±0.33	>100
8	49.6±7.4	9.46±1.41	0.82±0.12	>100
Iproniazid phosphate	13.3±2.0	—	—	—
HupA	—	2.24±0.34	—	—
PI103	—	—	0.09±0.01	—
L-Cysteine	—	—	—	27.8±4.2

[a]Each data point was the average value of three experimental measurements.
[b]Iproniazid phosphate, HupA (Huperzine A), PI103 (PI3K/mTOR inhibitor), and L-Cysteine were used as positive controls for anti-biological target agents.
[c]Concentrations exceeding 100 μM exhibited no significant inhibitory activity and are denoted as >100 μM.

EXPERIMENTAL

Fungus material

The experimental strain *Trichoderma koningiopsis* YN-G-1 used in this study was isolated from surface-sterilized roots of *Taxus yunnanensis* and was identified through an integrated approach combining morphological characterization and next-generation sequencing (NGS) technology. Initial morphological identification was performed based on colony characteristics and conidial morphology observed on PDA medium. Subsequent high-throughput sequencing of the ITS region was conducted using the Illumina platform. Bioinformatics analysis against the UNITE database revealed > 99% sequence similarity with the reference strain CBS 119075. The ITS sequence of this strain has been deposited in the GenBank database (Accession No. OK414029).

General experimental procedures

The ^{13}C-NMR and ^{1}H-NMR spectra were acquired on a Bruker AM-600 spectrometer (600 MHz). Macroporous resin (HPD-100) was obtained from Tianjin Haoju Resin Technology Co., Ltd., while column chromatography silica gel (200–300 mesh) and TLC silica gel GF254 were purchased from Shanxi Nuotai Biotechnology Co., Ltd. High-performance liquid chromatography (HPLC) was performed using a system from Jiangsu Hanbang Technology equipped with a YMC-Pack (USA) column (250 mm × 10 mm, 5 μm).

Extraction and isolation

The strain YN-G-1 was cultured in rice medium (80 g rice plus 100 mL sterilized water per 500 mL Erlenmeyer flask, totaling 60 bottles) at 28 °C with 80% relative humidity for 40 days. After fermentation, the products were dried, crushed, and extracted with ethyl acetate (3 × 2000 mL) to yield 20.0 g of crude extract. The extract was first fractionated by macroporous resin column chromatography using a stepwise ethanol-water gradient (0 → 90% v/v), yielding four fractions (A-D). Fraction A was subjected to silica gel column chromatography with a petroleum ether-acetone gradient (20:1 → 2:1 v/v), producing three subfractions: A-a (500.0 mg)

was further purified by silica gel CC (petroleum ether-acetone 10:1 → 2:1 v/v) to yield compound **7** (10.0 mg); A-b (160.0 mg) was purified by HPLC (MeOH-H_2O 75:25 v/v, 1.2 mL/min, 254 nm) to afford compound **1** (5.0 mg, tR = 19.0 min); and A-c (380.0 mg) was processed by silica gel CC (petroleum ether-acetone 8:1 → 2:1 v/v) to give compound **2** (10.0 mg). Fraction B was separated by silica gel CC (petroleum ether-acetone 20:1 → 2:1 v/v) into B-a (140.0 mg), which was purified by HPLC (MeOH-H_2O 60:40 v/v, 1.5 mL/min, 254 nm) to obtain compound **3** (3.0 mg, tR = 23.0 min), and B-b (120.0 mg), which yielded compound **4** (5.0 mg) after silica gel CC (petroleum ether-ethyl acetate 20:1 → 6:1 v/v). Fraction C was fractionated by silica gel CC (petroleum ether- ethyl acetate 20:1 → 1:1 v/v) to give C-a (810.0 mg), which was further purified to yield compound **5** (6.0 mg), and C-b (150.0 mg), which afforded compound **6** (5.2 mg). Finally, fraction D was directly purified by silica gel CC (petroleum ether- ethyl acetate 30:1 → 1:1 v/v) to isolate compound **8** (6.1 mg).

Koninginin A (**1**), ESI-MS *m/z* 285 $[M + H]^+$; ^{1}H-NMR (600 MHz, $CDCl_3$) δ_H 4.32 (1H, br s, H-9), 4.03 (1H, t, *J* = 7.0 Hz, H-10), 3.89 (1H, ddd, *J* = 11.3, 3.1, 5.0 Hz, H-1), 3.61 (1H, dd, *J* = 11.8, 4.4 Hz, H-4), 2.25 (1H, m, H-8b), 2.11 (1H, m, H-7a), 1.96 (1H, m, H-3b), 1.85 (1H, m, H-3a), 1.84 (1H, m, H-2b), 1.72 (1H, m, H-7b), 1.59 (1H, m, H-2a), 1.57 (1H, m, H-6), 1.53 (1H, m, H-11a), 1.51 (1H, m, H-8a), 1.48 (1H, m, H-11b), 1.33 (8H, m, H-12,13,14,15), 0.88 (3H, t, *J* = 6.9 Hz, H-16); ^{13}C-NMR (150 MHz, $CDCl_3$) δ_C 109.4 (C-5), 79.5 (C-10), 79.3 (C-9), 72.9 (C-1), 70.1 (C-4), 41.6 (C-6), 35.4 (C-11), 31.9 (C-14), 31.0 (C-2), 29.2 (C-13), 27.4 (C-8), 25.7 (C-12), 25.4 (C-3), 22.7 (C-15), 20.7 (C-7), 14.2 (C-16) [15].

Koninginin D (**2**),ESI-MS *m/z* 299 $[M + H]^+$; ^{1}H-NMR (600 MHz, CD_3OD) δ_H 4.67 (1H, s, H-7), 4.42 (1H, t, *J*=6.0 Hz, H-4), 4.17 (1H, ddd, *J* = 12.7, 4.4, 2.2 Hz, H-9), 3.71(1H, m, H-10), 2.65 (1H, ddd, *J* = 16.8, 8.6, 4.8 Hz, H-2b), 2.33 (1H, ddd, *J* = 16.8, 7.9, 4.7 Hz, H-2a), 2.20 (1H, m, H-3b), 2.02 (1H, m, H-3a), 1.90 (1H, dt, *J* = 14.2, 2.2 Hz, H-8b), 1.70 (1H, m, H-8a), 1.66 (2H, m, H-11), 1.57(2H, m, H-12), 1.37 (2H, m, H-13), 1.36 (2H, m, H-14), 1.35 (2H, m, H-15), 0.94 (3H, t, *J* = 6.8 Hz, H-16); ^{13}C-NMR (150 MHz, CD_3OD): δ_C 199.5 (C-1), 174.1 (C-5), 114.4 (C-6), 77.7 (C-9), 73.5 (C-10), 66.7 (C-4), 57.6 (C-7), 34.1 (C-2), 33.7 (C-11), 33.0 (C-14), 32.4 (C-8), 30.4 (C-13), 30.4 (C-3), 26.6 (C-12), 23.7 (C-15), 14.4 (C-16) [16].

Trichodermatides B (**3**), ESI-MS *m/z* 281 $[M + H]^+$; ^{1}H-NMR (600 MHz, $CDCl_3$) δ_H 5.25 (1H, m, H-9), 4.05 (1H, dd, *J*=13.1, 8.6 Hz, H-2), 3.12-2.63 (3H, m, H-8, 7α), 2.58-2.38 (5H, m, H-4, 11, 7β), 2.32 (1H, m, H-3α), 1.84 (1H, m, H-3β), 1.54 (2H, m, H-12), 1.26 (6H, br s, H-13, 14, 15), 0.83 (3H, t, *J*=6.8 Hz, H-16); ^{13}C-NMR (150 MHz, $CDCl_3$): δ_C 207.4 (10-CO), 195.1(1-CO), 177.8 (C-5), 110.6 (C-6), 82.3 (C-9), 71.5 (C-2), 48.4 (C-8), 43.5 (C-11), 31.7 (C-7), 31.6 (C-14), 30.1 (C-3), 29.0 (C-13), 23.5 (C-12), 22.9 (C-4), 22.5 (C-15), 14.0 (C-16) [17].

Trichodermaketones C (**4**), ESI-MS m/z 287 $[M + Na]^+$; ^{1}H-NMR (600 MHz, $CDCl_3$) δ_H 5.80 (1H, dt, *J*=15.1, 6.8 Hz, H-10), 5.58 (1H, dd, *J*=15.1, 9.9 Hz, H-9), 5.21 (1H, m, H-8), 4.57 (1H, t, *J*=6.6 Hz, H-4), 2.98 (1H, dd, *J*=14.8, 9.9 Hz, H-7a), 2.61 (1H, dd, *J*=14.8, 7.8 Hz, H-7b), 2.54 (1H, dt, *J*=11.4, 5.8 Hz, H-2a), 2.36 (1H, dt, *J*=11.4, 5.6 Hz, H-2b), 2.24 (1H, m, H-3a), 2.05 (2H, m, H-11), 2.01 (1H, m, H-3b), 1.37 (2H, m, H-12), 1.28 (6H, br s, H-13, 14, 15), 0.87 (3H, t, *J*=6.8 Hz, H-16); ^{13}C-NMR (150 MHz, $CDCl_3$) δ_C 195.1 (1-CO), 175.1 (C-5), 136.4 (C-10), 127.8 (C-9), 113.1 (C-6), 87.5 (C-8), 63.8 (C-4), 34.8 (C-2), 32.5 (C-7), 32.2 (C-11), 31.8(C-13), 31.0 (C-3), 28.9 (C-12), 28.8 (C-14), 22.7 (C-15), 14.2 (C-16) [18].

Koninginin B (**5**), ESI-MS *m/z* 305 $[M + Na]^+$; ^{1}H-NMR (600 MHz, $CDCl_3$) δ_H 4.05 (1H, dd, *J* = 13.1, 5.4 Hz, H-2), 3.78 (1H, ddd, *J* = 11.3, 5.0, 2.1 Hz, H-9), 3.64 (1H, dt, *J* = 7.7, 5.0 Hz, H-10), 2.60(1H, m, H-4b), 2.46 (1H, m, H-4a), 2.36 (1H, m, H-3a), 2.05 (3H, m, H-7, H-8a), 1.79 (1H, m, H-3b), 1.63(3H, m, H-8b, H-11), 0.89 (3H, t, *J* = 6.8 Hz, H-16); ^{13}C-NMR (150 MHz, $CDCl_3$) δ_C 198.2 (1-CO), 171.4 (C-5), 109.3 (C-6), 80.9 (C-9), 73.3 (C-10), 71.2 (C-2), 32.9 (C-11), 31.9 (C-14), 29.4 (C-15), 29.1 (C-3), 27.3 (C-4), 25.5 (C-12), 22.8 (C-8), 22.7 (C-15), 17.8 (C-7), 14.2 (C-16) [19].

Ergosterol peroxide (**6**), ^{1}H-NMR (600 MHz, $CDCl_3$): δ_H 6.50 (1H, d, *J* = 8.5 Hz, H-7), 6.25 (1H, d, *J* = 8.5 Hz, H-6), 5.23 (1H, dd, *J* = 15.2, 7.7 Hz, H-23), 5.14 (1H, dd, *J* = 15.2, 8.4 Hz, H-

22); δ_H 3.97(1H, m, H-3); δ_H 0.99 (3H, d, *J* = 6.6 Hz, H-21), 0.89(6H, m, H-28, 19), 0.82 (9H, m, H-27, 18, 26) [20].

p-Hydroxyphenyl-*β*-ethanol (**7**), ESI-MS *m/z* 139 $[M + H]^+$; ^{1}H-NMR (600 MHz, MeOD) δ_H 7.04 (2H, d, *J* = 8.4 Hz, H-1, 5), 6.71 (2H, d, *J* = 8.4 Hz, H-2, 4), 3.69 (2H, t, *J* = 7.2 Hz, H-8), 2.72 (2H, t, *J* = 7.2 Hz, H-7); ^{13}C-NMR (150 MHz, MeOD) δ_C 156.7 (C-3), 131.0 (C-6), 130.9 (C-1, 5), 116.1 (C-2, 4), 64.6 (C-8), 39.4 (C-7) [21].

Drechslerol-B (**8**), ESI-MS *m/z* 605 $[M + H]^+$; ^{1}H-NMR (600 MHz, $CDCl_3$): δ_H 5.35 (4H, m, H-16, 17, 31, 32), 4.28 (2H, t , *J* = 7.0 Hz, H-21), 4.14 (1H, m, H-23), 2.05 (2H, m, H-22), 1.27 (60H, m, 30×CH_2), 0.87 (6H, t, *J* = 6.8 Hz, H-1, 40); ^{13}C-NMR (150 MHz, $CDCl_3$): δ_C 173.4 (20-CO), 130.3 (C-16, 17), 129.8 (C-31, 32), 69.0 (C-23), 62.2 (C-21), 34.2-22.7 (31×C), 14.2 (C-1, 40) [22].

Bioassays

The inhibitory activities against MAO, AChE, and PI3K were evaluated following the previously established protocol [31-36], while PDE1 activity was determined via a UV spectrophotometric assay [37]. This assay relies on the enzymatic conversion of thymidine 5-monophosphate p-nitrophenyl ester sodium salt to p-nitrophenol, a yellow chromogenic product with maximal absorbance at 405 nm, where inhibitory potency is quantified by absorbance changes: reduced product formation (lower absorbance) indicates stronger inhibition, and higher absorbance reflects weaker inhibition. The assay system, conducted in a 96-well microplate, included a blank control (160.0 µL Tris-HCl buffer, pH 8.9, prepared by dissolving 133.2 mg Tris (hydroxymethyl) aminomethane in 9.0 mL deionized water with 64.35 mg NaCl, 14.28 mg $MgCl_2$, pH-adjusted using HCl, and volumetrically standardized to 10 mL), a complete inhibition group (140.0 µL Tris-HCl buffer + 20.0 µL 100.0 µg/mL L-cysteine stock solution, prepared at 10.0 mg/mL and proportionally diluted), a positive control group (140.0 µL Tris-HCl buffer + 20.0 µL serially diluted L-cysteine, 0.001– 0.012 mg/mL), a sample group (140.0 µL Tris-HCl buffer + 20.0 µL test compound solution), and background controls (160.0 µL Tris-HCl buffer + 20.0 µL corresponding test/control solutions). Following reagent addition, plates were incubated at 4 °C for 20 min. Reactions were then initiated by adding 0.65 mM substrate (dissolved in DMSO; 20.0 µL/well, final DMSO concentration 0.5% v/v) and incubated at 45 °C for 15 min. Absorbance at 405 nm was measured in triplicate using a microplate reader. The inhibition percentage was calculated using the equation: Inhibition (%) = [(Blank absorbance − Positive Control absorbance) − (Test absorbance − Positive Control absorbance)] / (Blank absorbance − Positive Control absorbance) × 100, where Blank absorbance, Positive Control absorbance, and Test absorbance represent the absorbance values of the blank, positive control, and test groups, respectively. IC_{50} were derived through non-linear regression analysis of concentration-response curves using GraphPad Prism software.

CONCLUSION

This study examined the metabolic products of the fungus *Trichoderma koningiopsis* YN-G-1, isolating five polyketides, one sterol, one phenolic derivative, and one ester compound. These findings expand the known chemical diversity of this fungal species. The polyketides are particularly noteworthy, as previous studies on related fungi suggest these compounds may help to protect nerve cells. The structural analysis of these compounds provides a foundation for future drug research. Their potential nerve-protecting effects align with findings in similar fungi, possibly offering clues for developing treatments for neurodegenerative diseases. This work highlights the value of studying fungal resources, which can deepen our knowledge of microbial chemistry and reveal useful natural compounds. These findings enhance the research significance of *T. koningiopsis*, warranting further investigation into its mechanisms and practical applications.

ACKNOWLEDGEMENTS

This work was supported by the National Natural Science Foundation of China (No. 22267011), the Industrial support plan project of colleges and universities in Gansu Province (No. 2022CYZC-29), the project of the Bureau of Science and Technology of Lanzhou (2023-RC-43) and Science and Technology Plan Project of Wenzhou, China (Y20220198).

REFERENCES

1. Mill, R.R.; Banks, L.; Brickell, C. Diversity in Strategies for conifer conservation, the action plan and future developments. *Acta Hortic.* **2003,** 6, 397-403.
2. Yan, C.; Yin, Y.; Zhang, D.; Yang, W.; Yu, R. Structural characterization and in vitro antitumor activity of a novel polysaccharide from *Taxus yunnanensis*. *Carbohydr. Polym.* **2013**, 96, 389-395.
3. Stierle, A.; Strobel, G.; Stierle, D. Taxol and taxane production by *Taxomyces andreanae*, an endophytic fungus of Pacific yew. *Sci.* **1993**, 260, 214-216.
4. Kharwar, R.N.; Mishra, A.; Gond, S.K.; Stierle, A.; Stierle, D. Anticancer compounds derived from fungal endophytes: Their importance and future challenges. *Nat. Prod. Rep.* **2011**, 28, 1208-1228.
5. Wilson, Z.; Brimble, M. Molecules derived from the extremes of life. *Nat. Prod. Rep.* **2009**, 26, 44-71.
6. Tan, R.X.; Zou, W.X. Endophytes: A rich source of functional metabolites. *Nat Prod. Rep.* **2001**, 18, 448-459.
7. Chen, H.W.; Jiang, C.X.; Ma, G.L.; Wu, X.Y.; Jiang, W.; Li, J.; Zang, Y.; Li, J.; Xiong, J.; Hu, J.F. Unprecedented spirodioxynaphthalenes from the endophytic fungus *Phyllosticta ligustricola* HDF-L-2 derived from the endangered conifer *Pseudotsuga gaussenii*. *Phytochemistry* **2023**, 211, 113687-113695.
8. Vu, T.H.N.; Pham, N.; Quach, N.T.; Ngo, C.; Chu, H.; Phi, Q.T. Fusarium foetens AQF6 Isolated from *Amentotaxus yunnanensis* H.L.Li as a prolific source of antioxidant compounds. *Appl. Sci.* **2024**, 14, 1-12.
9. Zhu, F.; Qin, C.; Tao, L.; Liu, X.; Shi, Z.; Ma, X.; Jia, J.; Tan, Y.; Cui, C.; Lin, J.; Tanl, C.; Jiang, Y.; Chen, Y. Clustered patterns of species origins of nature-derived drugs and clues for future bioprospecting. *Proc. Natl. Acad. Sci. U S A.* **2011**, 108, 12943-12948.
10. Zhang, H.W.; Song, Y.C.; Tan, R.X. Biology and chemistry of endophytes. *Nat. Prod. Rep.* **2006**, 23, 753-771.
11. Leylaie, S.; Zafari, D. Antiproliferative and antimicrobial activities of secondary metabolites and phylogenetic study of Endophytic *Trichoderma* species from *Vinca* plants. *Front. Microbiol.* **2018**, 9, 1484-1488.
12. Liu, K.; Yang, Y.B.; Chen, J.L.; Miao, C.P.; Wang, Q.; Zhou, H.; Chen, Y.W.; Li, Y.Q.; Ding, Z.T.; Zhao, L.X. Koninginins N-Q, Polyketides from the endophytic fungus *Trichoderma koningiopsis* harbored in *Panax notoginseng*. *Nat. Prod. Bioprospect.* **2016**, 6, 49-55.
13. Shi, X.S.; Li, H.L.; Li, X.M.; Wang, D.J.; Li, X.; Meng, L.H.; Zhou, X.W.; Wang, B.G. Highly oxygenated polyketides produced by *Trichoderma koningiopsis* QA-3, an endophytic fungus obtained from the fresh roots of the medicinal plant *Artemisia argyi*. *Bioorg. Chem.* **2020**, 94, 103448-1034513.
14. Lang, B.Y.; Li, J.; Zhou, X.X.; Chen, Y.H.; Yang, Y.H.; Li, X.N.; Zeng, Y.; Zhao, P.J. Koninginins L and M, two polyketides from *Trichoderma koningii* 8662. *Phytochem. Lett.* **2015**, 11, 1-4.
15. Almassi, F.; Ghisalberti, E.L.; Narbey, M.J.; Sivasithamparam, K. New Antibiotics from strains of *Trichoderma harzianum*. *J. Nat. Prod.* **1991**, 54, 396-402.

16. Dunlop, R.W.; Simon, A.; Sivasithamparam, K.; Ghisalberti, E.L. An antibiotic from *Trichoderma koningii* active against soilborne plant pathogens. *J. Nat. Prod.* **1989,** 52, 67-74.
17. Sun, Y.; Tian, L.; Huang, J.; Ma, H.Y.; Zheng, Z.; Lv, A.L.; Yasukawa, K.; Pei, Y.H. Trichodermatides A-D, novel polyketides from the marine-derived fungus *Trichoderma reesei*. *Org. Lett.* **2008**, 10, 393-396.
18. Song, F.H.; Dai, H.Q.; Tong, Y.J.; Ren, B.; Chen, C.X.; Sun, N.; Liu, X.Y.; Bian, J.; Liu, M.; Gao, H.; Liu, H.W.; Chen, X.P.; Zhang, L.X. Trichodermaketones A−D and 7-O-methylkoninginin D from the marine fungus *Trichoderma koningii*. *J. Nat. Prod.* **2010**, 73, 806-810.
19. Liu, G.; Wang, Z. Total synthesis of koninginin D, B and E. *Synthesis* **2001**, 201, 119-127.
20. Hybelbauerová, S.; Sejbal, J.; Dracínský, M.; Hahnová, A.; Koutek, B. Chemical constituents of Stereum subtomentosum and two other birch-associated basidiomycetes: An interspecies comparative study. *Chem. Biodivers.* **2008**, 5, 743-750.
21. Huang, Q.; Tezuka, Y.; Hatanaka, Y.; Kikuchi, T.; Nishi, A.; Tubaki, K. Studies on metabolites of Mycoparasitic Fungi. III. New sesquiterpene alcohol from *Trichoderma koningii*. *Chem. Pharm. Bull.* **1995**, 43, 1035-1038.
22. Shukla, R.S.; Agrawal, K.; Thakur, R.S.; Husain, A. Drechslerol-B, A host-selective phytotoxin produced by *Drechslera maydis*. *Phytochemistry* **1989,** 28, 2089-2091.
23. Cutler, H.G.; Himmelsbach, D.S.; Arrendale, R.F.; Cole, P.D.; Cox, R.H. Koninginin A: A novel plant growth regulator from *Trichoderma koningii*. *Agric. Biol. Chem.* **1989**, 53, 2605-2611.
24. Cutler, H.G.; Himmelsbach, D.S.; Yagen, B.; Arrendale, R.F.; Jacyno, J.M.; Cole, P.D.; Cox, R.H. Koninginin B: A biologically active congener of koninginin A from *Trichoderma koningii*. *J. Agric. Food. Chem*. **1991**, 39, 977-980.
25. Tezuka, Y.; Tasaki, M.; Huang, Q.; Hatanaka, Y.; Kikuchi, T. Studies on metabolites of Mycoparasitic fungi, 6. 15-hydroxyacorenone: New acorane-type sesquiterpene from the culture broth of the mycoparasitic fungus *Trichoderma harzianum*. *Liebigs Annalen.* **1997**, 12, 2579-2580.
26. Chen, K.; Yang, H.T.; Li, J.S.; Zhang, G.Z.; Huang, Y.J.; Zhao, X.Y. Bioactive secondary metabolites of polyketides from Trichoderma. *Chin. J. Biol. Control.* **2009**, 25, 171-178.
27. Herraiz, T.; González, D.; Azpilicueta, C.A.; Arán, V. J.; Guillén, H. β-Carboline alkaloids in *Peganum harmala* and inhibition of human monoamine oxidase. *Food. Chem. Toxicol.* **2010**, 48, 839-845.
28. Houghton, P.J.; Ren, Y.; Howes, M.J. Acetylcholinesterase inhibitors from plants and fungi. *Nat. Prod. Rep.* **2006**, 23, 181-199.
29. Stephens, L.; Williams, R.; Hawkins, P. Phosphoinositide 3-kinases as drug targets in cancer. *Curr. Opin.Pharmacol.* **2005**, 5, 357-365.
30. Chan, S.; Yan, C. PDE1 isozymes, key regulators of pathological vascular remodeling. *Curr. Opin. Pharmacol.* **2011**, 11, 720-724.
31. Zhi, K.K.; Yang, Z.D.; Shi, D.F.; Yao, X.J.;Wang, M.G. Desmodeleganine, a new alkaloid from the leaves of *Desmodium elegans* as a potential monoamine oxidase inhibitor. *Fitoterapia.* **2014**, 98, 160-165.
32. Wu, S.Y.; Chen, X.Q.; Ren, J.L.; Liu, P.L.; Yan, Q.; Chen, Z.M. Cuparene-type sesquiterpenes with neuroprotective activities from the edible mushroom *Flammulina filiformis*. *Fitoterapia*. **2024**, 179, 10235-10245.
33. Salleh, W.M.N.H.W.; Nafiah, M.A.; Yen, K.H.; Kassim, H.; Tawang, A. Chemical constituents and acetylcholinesterase inhibitory activity of *Piper abbreviatum* Opiz. *Bull. Chem. Soc. Ethiop.* **2021**, 34, 625-632.
34. Salleh, W.M.N.H.W.; Hashim, N.A.; Khamis, S. Chemical constituents and lipoxygenase inhibitory activity of *Piper stylosum* Miq. *Bull. Chem. Soc. Ethiop.* **2019**, 33, 587-592.

35. Yang, Z.D.; Duan, D.Z.; Xue, W.W.; Yao, X.J.; Li, S. Steroidal alkaloids from *Holarrhena antidysenterica* as acetylcholinesterase inhibitors and the investigation for structure–activity relationships. *Life Sci.* **2012**, 90, 929-933.
36. Zhao, J.W.; Yang, Z.D.; Zhou, S.Y.; Yang, L.J.; Sun, J.H.; Yao, X.J.; Shu, Z.M.; Li, S. Wortmannine F and G, two new pyranones from *Talaromyces wortmannii* LGT-4, the endophytic fungus of *Tripterygium wilfordii*. *Phytochem. Lett.* **2019**, 29, 115-118.
37. Garbagna, L.; Cojazzi, M.; Mussini, E. A Spectrophotometry assay of phosphodiesterases. *Anal. Lett.* **1980**, 13, 683-689.